




Zinc Toxicity and Iron-Sulfur Cluster Biogenesis in *Escherichia coli*

Jianghui Li,^a Xiaojun Ren,^b Bingqian Fan,^b Zhaoyang Huang,^b Wu Wang,^a Huaibin Zhou,^b Zhefeng Lou,^b  Huangeng Ding,^c Jianxin Lyu,^b Guoqiang Tan^a

^aLaboratory of Molecular Medicine, Zhejiang Provincial Key Laboratory for Technology and Application of Model Organisms, Key Laboratory of Laboratory Medicine, Ministry of Education, China, School of Laboratory Medicine and Life Sciences, Wenzhou Medical University, Wenzhou, Zhejiang, China

^bZhejiang Provincial Key Laboratory of Medical Genetics, Key Laboratory of Laboratory Medicine, Ministry of Education, China, School of Laboratory Medicine and Life Sciences, Wenzhou Medical University, Wenzhou, Zhejiang, China

^cDepartment of Biological Sciences, Louisiana State University, Baton Rouge, Louisiana, USA

ABSTRACT While zinc is an essential trace metal in biology, excess zinc is toxic to organisms. Previous studies have shown that zinc toxicity is associated with disruption of the [4Fe-4S] clusters in various dehydratases in *Escherichia coli*. Here, we report that the intracellular zinc overload in *E. coli* cells inhibits iron-sulfur cluster biogenesis without affecting the preassembled iron-sulfur clusters in proteins. Among the housekeeping iron-sulfur cluster assembly proteins encoded by the gene cluster *iscSUA-hscBA-fdx-iscX* in *E. coli* cells, the scaffold IscU, the iron chaperone IscA, and ferredoxin have strong zinc binding activity in cells, suggesting that intracellular zinc overload inhibits iron-sulfur cluster biogenesis by binding to the iron-sulfur cluster assembly proteins. Mutations of the conserved cysteine residues to serine in IscA, IscU, or ferredoxin completely abolish the zinc binding activity of the proteins, indicating that zinc can compete with iron or iron-sulfur cluster binding in IscA, IscU, and ferredoxin and block iron-sulfur cluster biogenesis. Furthermore, intracellular zinc overload appears to emulate the slow-growth phenotype of the *E. coli* mutant cells with deletion of the iron-sulfur cluster assembly proteins IscU, IscA, and ferredoxin. Our results suggest that intracellular zinc overload inhibits iron-sulfur cluster biogenesis by targeting the iron-sulfur cluster assembly proteins IscU, IscA, and ferredoxin in *E. coli* cells.

IMPORTANCE Zinc toxicity has been implicated in causing various human diseases. High concentrations of zinc can also inhibit bacterial cell growth. However, the underlying mechanism has not been fully understood. Here, we report that zinc overload in *Escherichia coli* cells inhibits iron-sulfur cluster biogenesis by targeting specific iron-sulfur cluster assembly proteins. Because iron-sulfur proteins are involved in diverse physiological processes, the zinc-mediated inhibition of iron-sulfur cluster biogenesis could be largely responsible for the zinc-mediated cytotoxicity. Our finding provides new insights on how intracellular zinc overload may inhibit cellular functions in bacteria.

KEYWORDS IscA, IscU, ferredoxin, iron-sulfur proteins, zinc toxicity

As an essential trace element, zinc is vitally important for all living organisms (1). At least 300 enzymes in the metabolic pathways of sugars, lipids, proteins, and nucleic acids use zinc as a cofactor (2). Lack of zinc has been attributed to many human health complications, including growth retardation, poor appetite, and cell-mediated immune dysfunction (3). On the other hand, excess zinc is highly toxic to cells (4–6). For example, an elevated intracellular zinc content has been linked to Alzheimer's disease (7) and Kufor-Rakeb syndrome (juvenile Parkinsonism) (8). In *Escherichia coli* cells,

Citation Li J, Ren X, Fan B, Huang Z, Wang W, Zhou H, Lou Z, Ding H, Lyu J, Tan G. 2019. Zinc toxicity and iron-sulfur cluster biogenesis in *Escherichia coli*. *Appl Environ Microbiol* 85:e01967-18. <https://doi.org/10.1128/AEM.01967-18>.

Editor Alfons J. M. Stams, Wageningen University

Copyright © 2019 Li et al. This is an open-access article distributed under the terms of the [Creative Commons Attribution 4.0 International license](https://creativecommons.org/licenses/by/4.0/).

Address correspondence to Jianxin Lyu, jxlu313@163.com, or Guoqiang Tan, tgq@wmu.edu.cn.

J. Li and X. Ren contributed equally to this work.

Received 13 August 2018

Accepted 1 February 2019

Accepted manuscript posted online 1 March 2019

Published 18 April 2019

intracellular total zinc accumulates to about 0.2 mM when cells are grown in LB medium (9). Radioactive ^{65}Zn -labeling studies (10) and proteomic analyses (11) have revealed a large number of putative zinc-binding proteins in *E. coli* cells. On the other hand, the addition of 2.5 mM ZnSO_4 to LB medium (12) or 0.35 mM ZnSO_4 to M9 minimum medium (13) completely inhibits *E. coli* cell growth. Because of the zinc-mediated inhibition of cell growth, zinc compounds have been developed as antibacterial agents and preservatives. Furthermore, host-mediated zinc toxicity to pathogenic bacteria has been extensively investigated (14–16). However, the molecular mechanism underlying the zinc-mediated cytotoxicity has not been fully understood.

Our previous studies have shown that topoisomerase I (17, 18) and its homolog YrdD (19) are iron and zinc binding proteins, and excess zinc can easily compete for iron binding in the proteins *in vivo* (17, 19). This suggests that zinc and iron may have similar binding sites in proteins.

In the past decade, several “zinc finger” proteins have been identified as iron-sulfur proteins. For example, the mitochondrial outer membrane protein mitoNEET (20) and the cleavage and polyadenylation specificity factor 30 (CPSF30) (21) have a zinc finger motif which hosts an iron-sulfur cluster. Since zinc and iron-sulfur cluster have similar ligand coordination in proteins, it has been proposed that zinc may compete for iron-sulfur center binding sites in proteins and disrupt iron-sulfur clusters in proteins (22–24). Since iron-sulfur proteins are involved in diverse physiological functions (25), excess zinc may affect multiple cellular functions by disrupting iron-sulfur clusters in proteins.

Iron-sulfur clusters are assembled by a group of dedicated proteins. In *E. coli*, there are two iron-sulfur cluster assembly systems encoded by the housekeeping *iscSUA-hscBA-fdx-iscX* gene cluster (26) and the inducible *sufABCDSE* gene cluster (22). Among the proteins encoded by *iscSUA-hscBA-fdx-iscX*, IscS is a cysteine desulfurase that provides sulfur for iron-sulfur cluster assembly (27). IscU is a scaffold protein that assembles iron-sulfur clusters (28) and transfers the transient clusters to target proteins (29, 30). IscA was thought to be an alternative scaffold (31). However, unlike the scaffold IscU, IscA has strong iron binding activity, and the iron center in IscA can be transferred to IscU for iron-sulfur cluster assembly (32–34). Thus, IscA is proposed as an iron chaperone for iron-sulfur cluster biogenesis. HscB and HscA are heat shock cognate proteins, which assist the iron-sulfur cluster transfer from IscU to target protein (35). Ferredoxin (Fdx) is a [2Fe-2S] cluster protein and may provide electrons for the iron-sulfur cluster assembly process (36). IscX has also been proposed as an iron donor for iron-sulfur cluster biogenesis (37). However, IscX has low iron binding affinity and interacts with IscS (38). The deletion of IscX does not significantly affect iron-sulfur proteins in *E. coli* cells (39). Therefore, the specific function of IscX remains to be defined.

In this study, we find that zinc overload in *E. coli* cells inhibits iron-sulfur cluster biogenesis without affecting the preassembled clusters in proteins. Additional studies reveal that zinc has strong interaction with the iron-sulfur cluster assembly proteins IscU, IscA, and ferredoxin, leading to inhibition of iron-sulfur cluster biogenesis in *E. coli* cells.

RESULTS

Zinc overload selectively inactivates iron-sulfur enzymes in *E. coli* cells. In wild-type *E. coli* cells, the “free” intracellular zinc concentration is in the femtomolar range (9). Zinc homeostasis in *E. coli* cells is regulated primarily through a network of zinc influx and efflux pumps. The major zinc efflux system ZntA, a P-type ATPase transporter, is upregulated by the transcription factor ZntR when intracellular zinc concentration is high (40). The deletion of ZntA results in an *E. coli* strain that is hypersensitive to zinc (41). To explore the effect of intracellular zinc overload on iron-sulfur proteins in *E. coli* cells, we have constructed an *E. coli* mutant in which both the zinc efflux pump ZntA and the transcription factor ZntR were deleted. Table 1 shows that the deletion of ZntA and ZntR resulted in accumulation of intracellular zinc

TABLE 1 Zinc content of whole cells after zinc treatment

Strain	Mean \pm SD zinc content (μM) of whole cells (per 100 OD at 600 nm)
MC4100	21.6 \pm 0.6
MC4100+Zn	24.4 \pm 4.2
<i>zntA zntR</i> mutant	25.1 \pm 0.4
<i>zntA zntR</i> mutant + Zn	59.4 \pm 2.4

in *E. coli* cells grown in LB medium supplemented with 200 μM ZnSO_4 under aerobic growth conditions. ZnSO_4 at 200 μM was chosen, as it inhibited cell growth of the *E. coli zntA zntR* double mutant in LB medium by about 50% and did not significantly affect the cell growth of wild-type *E. coli* (see Fig. S1 in the supplemental material).

To investigate the effect of zinc overload on iron-sulfur proteins in *E. coli*, we first utilized fumarases. There are three fumarases in *E. coli*, fumarase A and fumarase B, which require a [4Fe-4S] cluster for their catalytic activity (42); and fumarase C, which has no iron-sulfur clusters (43). Each fumarase was expressed in the *E. coli zntA zntR* mutant cells grown in LB medium supplemented with or without 200 μM ZnSO_4 under aerobic conditions. Figure 1 shows that the addition of ZnSO_4 (200 μM) to LB medium

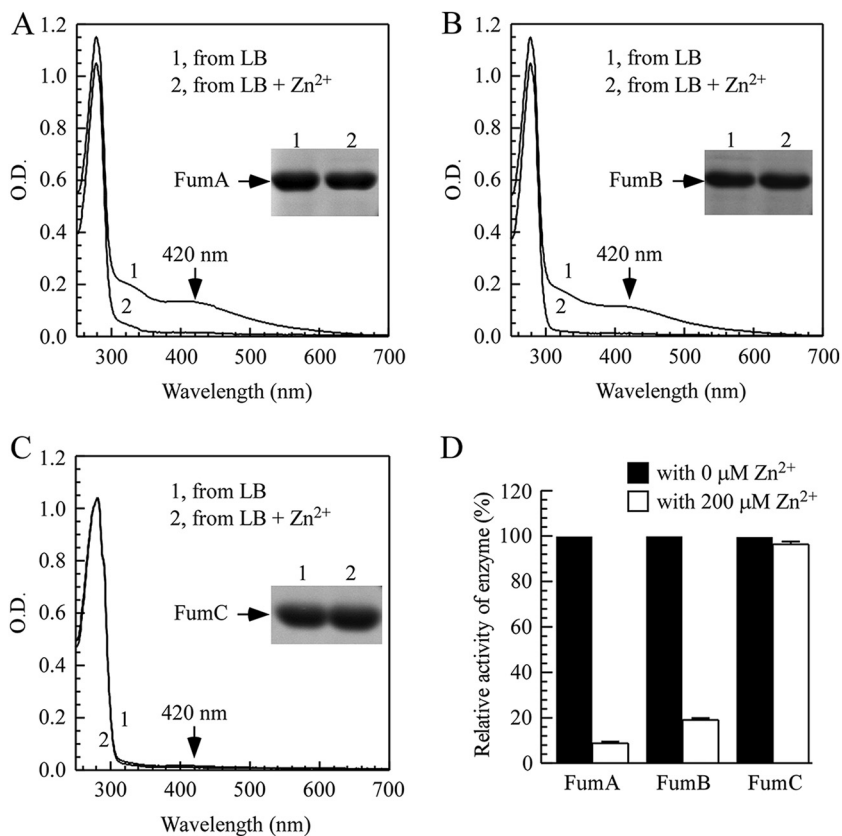


FIG 1 Zinc overload selectively inactivates iron-sulfur cluster containing fumarases by producing more apo forms. (A) UV-visible absorption spectra of recombinant fumarase A (FumA) proteins purified from *E. coli zntA zntR* double-mutant cells supplemented with 0 μM (spectrum 1) or 200 μM (spectrum 2) ZnSO_4 in LB medium. (B) UV-visible absorption spectra of recombinant fumarase B (FumB) proteins purified from *E. coli zntA zntR* double-mutant cells supplemented with 0 μM (spectrum 1) or 200 μM (spectrum 2) ZnSO_4 in LB medium. (C) UV-visible absorption spectra of recombinant fumarase C (FumC) proteins purified from *E. coli zntA zntR* double-mutant cells supplemented with 0 μM (spectrum 1) or 200 μM (spectrum 2) ZnSO_4 in LB medium. The inset in panels A to C is a photograph of the SDS-PAGE gel of purified proteins. (D) The relative fumarase activity of purified proteins from panels A to C. The relative activity is representative of the percentage of fumarase activity with 200 μM ZnSO_4 treatment in untreated samples. The results represent average \pm standard deviation from three independent experiments.

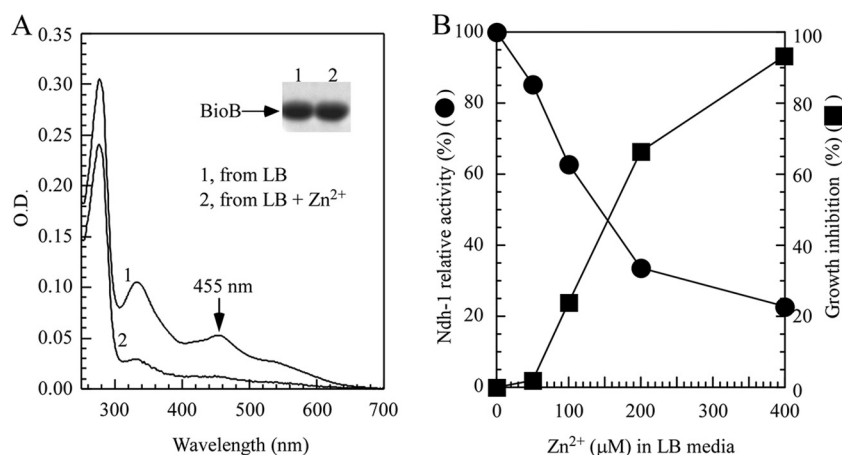


FIG 2 Excess zinc disrupts iron-sulfur cluster assembly in both [4Fe-4S] proteins and [2Fe-2S] proteins. (A) UV-visible absorption spectra of recombinant BioB purified from the *E. coli zntA zntR* double-mutant cells supplemented with 0 μM (spectrum 1) or 200 μM (spectrum 2) ZnSO_4 in LB medium under aerobic growth conditions. (B) Correlation of the relative activity of NADH dehydrogenase I and cell growth inhibition. The relative dehydrogenase I activity and relative cell growth were defined as the percentage of the *E. coli zntA zntR* double-mutant cells in LB medium with ZnSO_4 over that without ZnSO_4 . The relative cell growth inhibition rate was calculated by 100% minus the relative growth rate of the *E. coli zntA zntR* double-mutant cells. The relative dehydrogenase I activity (closed circles) and relative cell growth inhibition rate (closed squares) were plotted as a function of the ZnSO_4 concentration in LB medium. The 100% cell growth represented the cell density (OD at 600 nm) of ~ 3.0 after 5 h at 37°C in LB medium with aeration. The results were the most representative of three independent experiments.

largely eliminated the iron-sulfur cluster content (Fig. 1A and B) and the enzyme activity (Fig. 1D) of fumarases A and B in the *E. coli zntA zntR* mutant cells. On the other hand, the same zinc treatment did not affect the enzyme activity of fumarase C in *E. coli zntA zntR* mutant cells (Fig. 1C and D). The results suggested that zinc overload in *E. coli* cells selectively inhibits iron-sulfur cluster-containing fumarases A and B without inhibiting fumarase C, which does not have iron-sulfur clusters.

Effect of zinc overload on other iron-sulfur proteins in *E. coli* cells. To further explore the effects of zinc overload on iron-sulfur proteins, we used biotin synthase, which contains a [2Fe-2S] cluster and a [4Fe-4S] cluster (44). Biotin synthase (BioB) converts dethiobiotin into biotin by inserting a sulfur atom between C-6 and C-9 of dethiobiotin in an *S*-adenosylmethionine (SAM)-dependent reaction (45). In the experiments, recombinant BioB was expressed in the *E. coli zntA zntR* mutant cells grown in LB medium supplemented with or without 200 μM ZnSO_4 under aerobic conditions. Figure 2A shows that the addition of ZnSO_4 (200 μM) also decreased the iron-sulfur cluster contents of recombinant biotin synthase in the *E. coli zntA zntR* mutant cells.

We then analyzed the activity of the endogenous NADH dehydrogenase I, which contains multiple iron-sulfur clusters (46). Using deamino-NADH as a specific substrate for NADH dehydrogenase I (47), we found that the deamino-NADH oxidation rate of the *E. coli zntA zntR* mutant cells progressively decreased when the ZnSO_4 concentration in LB medium was gradually increased from 0 to 400 μM (Fig. 2B). The cell growth of the *E. coli zntA zntR* mutant was also inhibited as the ZnSO_4 concentration in LB medium was increased (Fig. 2B). Since the NADH dehydrogenase I contains multiple iron-sulfur clusters (48), the correlation between the decrease in the deamino-NADH oxidation rate and inhibition of cell growth by zinc in LB medium suggested that zinc toxicity could be closely associated with the inhibition of iron-sulfur proteins in *E. coli* cells.

Zinc overload inhibits iron-sulfur cluster biogenesis in *E. coli* cells. It was proposed that zinc may directly attack iron-sulfur clusters in proteins to produce the apo form in cells (22). On the other hand, zinc may block iron-sulfur cluster biogenesis, thus producing apo-form inactive proteins in cells. To delineate the two possibilities, we added ZnSO_4 (200 μM) to the *E. coli zntA zntR* mutant cells in LB medium before and after recombinant iron-sulfur protein was expressed.

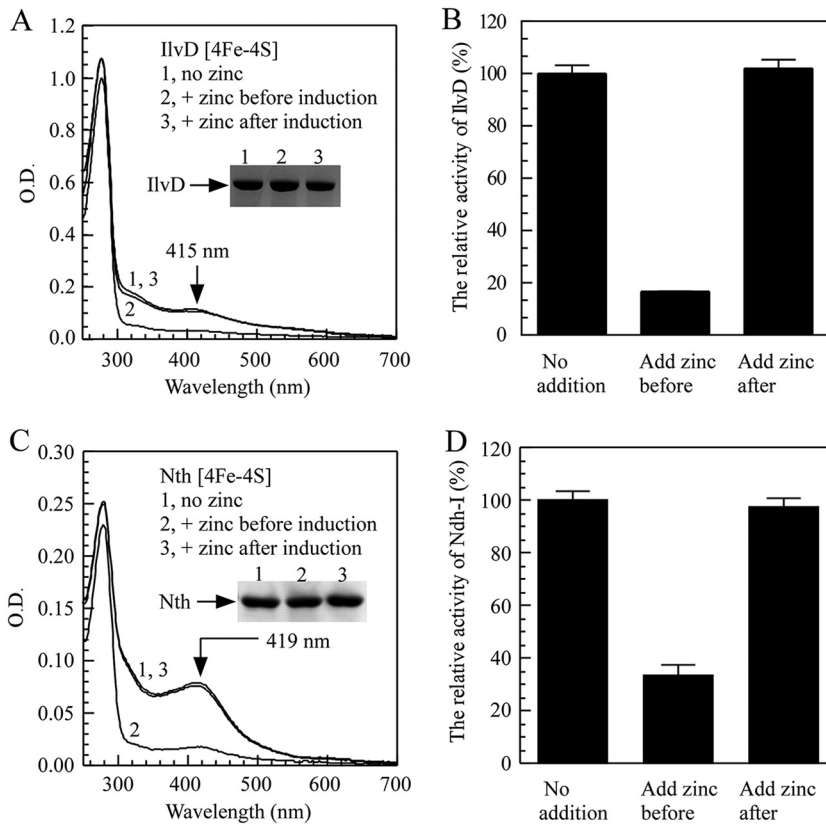


FIG 3 Excess zinc indirectly disrupts iron-sulfur cluster assembly in proteins. (A) Inhibition of the [4Fe-4S] cluster assembly in recombinant IlvD in the *E. coli* cells by zinc. UV-visible absorption spectra of recombinant IlvD purified from *E. coli zntA zntR* double-mutant cells supplemented with 0 μM (spectrum 1) or 200 μM ZnSO_4 grown in LB medium before (spectrum 2) and after (spectrum 3) protein was produced in the cells. The protein concentration of IlvD was 28 μM . The inset is a photograph of the SDS-PAGE gel of purified proteins. (B) Relative activity of purified IlvD from panel A. For the enzyme activity assay, 1 μM IlvD was used. The unit of IlvD enzyme activity referred to the production of keto acid (μM) per minute per micromolar IlvD. The relative activity of control sample was considered to be 100%, and the relative activity of other samples was obtained by dividing the control activity. (C) Inhibition of the [4Fe-4S] cluster assembly in recombinant endonuclease III (Nth) in the *E. coli* cells by zinc. UV-visible absorption spectra of recombinant endonuclease III (Nth) purified from *E. coli zntA zntR* double-mutant cells supplemented with 0 μM (spectrum 1) or 200 μM ZnSO_4 grown in LB medium before (spectrum 2) and after (spectrum 3) protein was produced in the cells. The protein concentration of IlvD was 12 μM . The inset is a photograph of the SDS-PAGE gel of purified proteins. (D) Effect of zinc on NADH dehydrogenase I in the *E. coli* cells. Inverted membrane vesicles (10 μl) were added to 290 μl reaction solution containing Tris (20 mM, pH 8.0), NaCl (200 mM), and deamino-NADH (50 μM). NADH dehydrogenase I activity was measured by monitoring the oxidation of deamino-NADH at 340 nm (extinction coefficient, 6.22 $\text{mM}^{-1} \text{cm}^{-1}$) at room temperature. The unit of NADH dehydrogenase I enzyme activity referred to the reduction of substrate (micromolar) per minute per OD at 600 nm. The relative activity of control sample was considered to be 100%, and the relative activity of other samples was obtained by dividing the control activity. The results represent average \pm standard deviation from three independent experiments.

In the experiment, recombinant dihydroxy-acid dehydratase (IlvD), which contains a [4Fe-4S] cluster for its enzyme activity in the branched-chain amino acid biosynthesis pathway (49), was expressed in the *E. coli zntA zntR* mutant cells grown in LB medium with or without ZnSO_4 (200 μM). IlvD was then purified from the cells. Figure 3A shows that the addition of ZnSO_4 (200 μM) to LB medium before recombinant IlvD was expressed largely eliminated iron-sulfur clusters in the protein. However, the addition of zinc to LB medium after IlvD was expressed did not significantly affect iron-sulfur clusters in the protein. The enzyme activity measurements further showed that zinc blocked iron-sulfur cluster assembly without affecting the preassembled iron-sulfur clusters in IlvD in the *E. coli* cells (Fig. 3B).

The recombinant endonuclease III (Nth), a DNA repair enzyme which hosts a stable [4Fe-4S] cluster (50), was also investigated. Figure 3C shows that while the addition of

ZnSO₄ (200 μM) to LB medium before endonuclease III was expressed in the *E. coli zntA zntR* mutant cells largely prevented iron-sulfur cluster assembly in the protein, the addition of ZnSO₄ (200 μM) to LB medium after endonuclease III was expressed did not significantly affect the preassembled iron-sulfur cluster in endonuclease III.

To further explore the inhibition of zinc overload on endogenous iron-sulfur cluster biogenesis, we measured the activity of the native NADH dehydrogenase I in the *E. coli* cells. Figure 3D shows that while the addition of ZnSO₄ (200 μM) to LB medium followed by 5 h of growth of the *E. coli zntA zntR* mutant cells significantly decreased the enzyme activity, the addition of ZnSO₄ (200 μM) to LB medium after 5 h of cell growth did not affect the enzyme activity of the NADH dehydrogenase I in the cells.

In *E. coli*, in addition to the housekeeping *iscSUA-hscBA-fdx-iscX* iron-sulfur gene cluster assembly system, there is another stress-inducible *sufABCDSE* system. Since increased expression of the gene cluster *sufABCDSE* is an indication of the iron-sulfur cluster assembly deficiency in *E. coli* cells (51, 52), we also analyzed the expression of the *sufA* operon in the *E. coli zntA zntR* mutant cells in response to ZnSO₄ in LB medium and found that expression of the *sufA* operon was indeed induced by ZnSO₄ treatment (Fig. S2B), suggesting that zinc has a general inhibitory effect on iron-sulfur cluster biogenesis in *E. coli* cells.

Taken together, the results suggested that ZnSO₄ (200 μM) inhibits iron-sulfur cluster biogenesis without affecting the preassembled iron-sulfur clusters in proteins in *E. coli* cells.

IscU, IscA, and ferredoxin are the major zinc targets among the housekeeping iron-sulfur cluster assembly machinery. The proteins encoded by *iscSUA-hscBA-fdx-iscX* represent the housekeeping iron-sulfur cluster biogenesis machinery in *E. coli* cells. If zinc inhibits iron-sulfur cluster biogenesis, it is possible that zinc may directly interact with iron-sulfur cluster assembly proteins. To test this idea, we expressed each protein encoded by the gene cluster *iscSUA-hscBA-fdx-iscX* in the *E. coli zntA zntR* mutant cells grown in LB medium supplemented or not with ZnSO₄ (200 μM). Purified proteins were then subjected to the UV-visible absorption measurements and metal content analyses.

Figure 4 shows that the addition of ZnSO₄ (200 μM) to LB medium had no effect on the UV-visible absorption spectra of IscS (Fig. 4A), IscU (Fig. 4B), HscB (Fig. 4D), HscA (Fig. 4E), and IscX (Fig. 4G) expressed in the *E. coli zntA zntR* mutant cells. On the other hand, the addition of ZnSO₄ (200 μM) to LB medium significantly decreased the iron binding peak at 315 nm of IscA (Fig. 4C) and the iron-sulfur cluster binding peaks at 415 nm and 459 nm of ferredoxin (Fig. 4F) expressed in the *E. coli zntA zntR* mutant cells, suggesting that zinc overload may block the iron binding in IscA and the iron-sulfur cluster binding in ferredoxin. The zinc content measurements in purified proteins (Fig. 4H) showed that IscU, IscA, and ferredoxin proteins contained 0.85 ± 0.16 , 0.94 ± 0.04 , and 1.69 ± 0.12 zinc atoms per protein monomer ($n = 3$), respectively. The stoichiometry of zinc binding in IscU is consistent with previous studies showing that each IscU monomer contains one zinc atom (24). On the other hand, other iron-sulfur cluster assembly proteins had only very little or no zinc binding (Fig. 4H). Thus, IscA, IscU, and ferredoxin are the major targets of zinc overload in the *E. coli zntA zntR* mutant cells.

The conserved cysteine residues in IscA, IscU, and ferredoxin are required for their zinc binding activity. To explore the zinc binding sites of IscU, IscA, and ferredoxin, we constructed an IscU mutant (IscU-3M) in which three cysteine residues (Cys-37, Cys-63, and Cys-106) were replaced with serine, an IscA mutant (IscA-3M) in which three cysteine residues (Cys-35, Cys-99, and Cys-101) were replaced with serine (48), and a ferredoxin mutant (Fdx-4M) in which four cysteine residues for binding the [2Fe-2S] cluster (Cys 42, Cys 48, Cys 51, and Cys 87) were replaced with serine. Wild-type IscU, IscA, and ferredoxin and their mutants (IscU-3M, IscA-3M, and ferredoxin-4M, respectively) were then expressed in the *E. coli zntA zntR* mutant cells grown in LB medium supplemented with increasing concentrations of ZnSO₄ (0 to 400 μM). Each protein was then purified from the *E. coli* cells.

Figure 5 shows that zinc binding in IscU, IscA, and ferredoxin was gradually increased in the *E. coli zntA zntR* mutant cells as the concentration of ZnSO₄ in LB

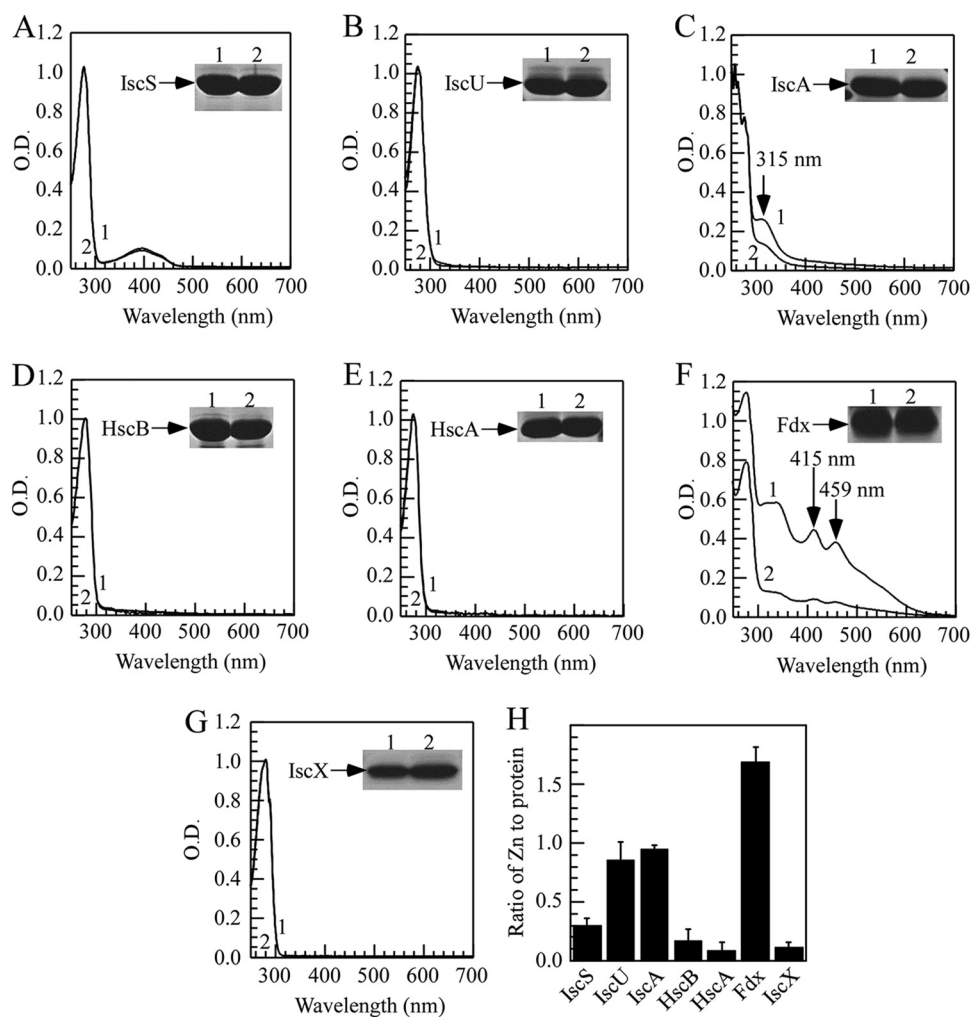


FIG 4 IscU, IscA, and ferredoxin are the major zinc binding proteins among the iron-sulfur cluster assembly proteins. Each protein encoded by the gene cluster *iscSUA-hscBA-fdx-iscX* was expressed in the *E. coli zntA zntR* double-mutant cells grown in LB medium supplemented or not with 200 μM ZnSO₄. Proteins were purified from the cells and subjected to UV-visible absorption measurements. (A) IscS. (B) IscU. (C) IscA. (D) HscB. (E) HscA. (F) Ferredoxin. (G) IscX. In each panel, spectrum 1 is without ZnSO₄ in LB medium, and spectrum 2 is with 200 μM ZnSO₄ in LB medium. The inset in each panel is a photograph of the SDS-PAGE gel of purified proteins. The results are representatives of three independent protein preparations. (H) The zinc content of the iron-sulfur cluster assembly proteins encoded by the gene cluster *iscSUA-hscBA-fdx-iscX* purified from the *E. coli zntA zntR* double-mutant cells grown in LB medium supplemented with 200 μM ZnSO₄. The results represent the average ± standard deviation from three independent experiments.

medium was increased. In contrast, the mutant proteins (IscU-3M, IscA-3M, and Fdx-4M) expressed in the *E. coli zntA zntR* mutant cells had very little or no zinc binding even after 400 μM ZnSO₄ was added to LB medium. Thus, IscU, IscA, and ferredoxin have specific zinc binding activity, and the conserved cysteine residues in IscU, IscA, and ferredoxin are essential for their zinc binding activity.

Zinc overload emulates the phenotype of an *E. coli* mutant with the deletion of IscU, IscA, and ferredoxin. If IscU, IscA, and ferredoxin are the major targets of zinc overload in the *E. coli* cells, the deletion of these genes would emulate the effects of zinc overload on iron-sulfur cluster biogenesis. To test this idea, we deleted the genes encoding IscU, IscA, and ferredoxin to produce an *E. coli iscU iscA fdx* mutant. Figure 6A shows that the deletion of IscU, IscA, and ferredoxin decreased the iron-sulfur cluster assembly in endonuclease III, which was similar to the inhibition of the iron-sulfur cluster assembly in endonuclease III in the *E. coli zntA zntR* mutant cells grown in LB medium supplemented with 200 μM ZnSO₄ (Fig. 6B). We also measured the cell growth

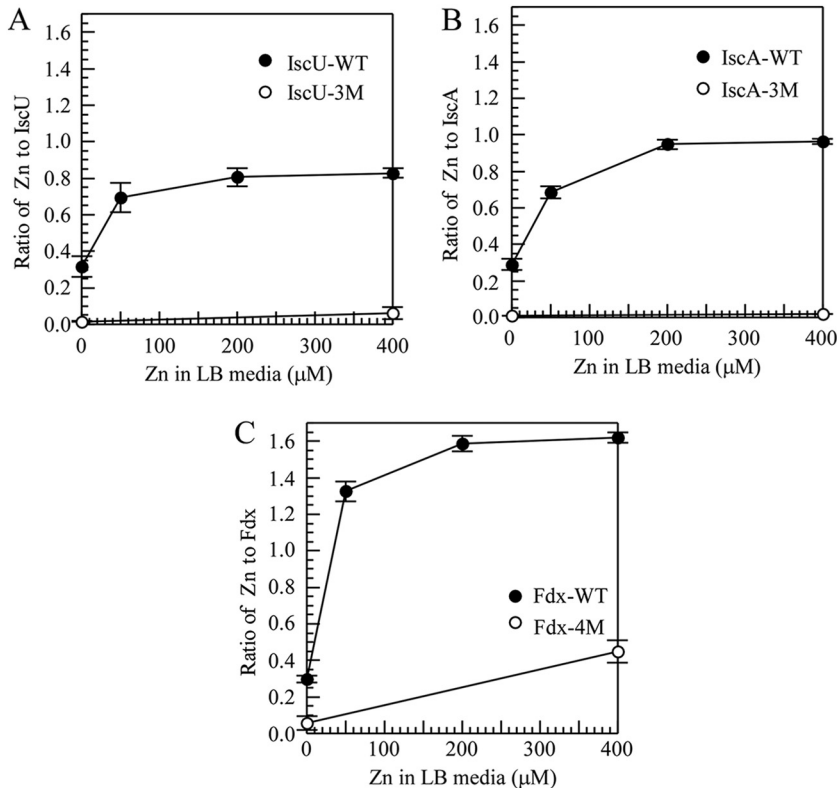


FIG 5 The conserved cysteine residues are required for the zinc binding activity for IscA, IscU, and ferredoxin. (A) Zinc binding activity of IscU in *E. coli zntA zntR* double-mutant cells in LB medium. Wild-type IscU and IscU mutant (IscU-3M) were expressed in *E. coli zntA zntR* double-mutant cells grown in LB medium supplemented with the indicated concentrations of $ZnSO_4$. Proteins were purified from *E. coli* cells and subjected to the zinc content analyses. Zinc content in purified IscU was plotted as a function of the $ZnSO_4$ concentration in LB medium. Closed circles, wild-type IscU; open circles, IscU-3M mutant. (B) Zinc binding activity of IscA in *E. coli zntA zntR* double-mutant cells in LB medium. Wild-type IscA and IscA mutant (IscA-3M) were expressed in *E. coli zntA zntR* double-mutant cells grown in LB medium supplemented with indicated concentrations of $ZnSO_4$. Proteins were purified from *E. coli* cells and subject to zinc content analysis. Zinc content in purified IscA was plotted as a function of the $ZnSO_4$ concentration in LB medium. Closed circles, wild-type IscA; open circles, IscA-3M mutant. (C) Zinc binding activity of ferredoxin in *E. coli zntA zntR* double-mutant cells in LB medium. Wild-type Fdx and an Fdx mutant (Fdx-4M) were expressed in *E. coli zntA zntR* double-mutant cells grown in LB medium supplemented with indicated concentrations of $ZnSO_4$. Proteins were purified from *E. coli* cells and subject to zinc content analysis. Zinc content in purified Fdx was plotted as a function of the $ZnSO_4$ concentration in LB medium. Closed circles, wild-type Fdx; open circles, Fdx-4M mutant. The results represent the average \pm standard deviation from three independent experiments.

of the *E. coli* mutant with the deletion of IscA, IscU, and ferredoxin and found that those deletions resulted in slow growth (Fig. 6C), which was also similar to that of the *E. coli zntA zntR* mutant cells grown in LB medium supplemented with 200 μM $ZnSO_4$ (Fig. 6D). Thus, zinc overload in *E. coli* cells appears to emulate the phenotype of the *E. coli* mutant cells with deletion of the iron-sulfur cluster assembly proteins IscU, IscA, and ferredoxin.

DISCUSSION

In this study, we report that zinc overload in the *E. coli zntA zntR* mutant cells inhibits iron-sulfur cluster biogenesis without affecting the preassembled iron-sulfur clusters in proteins or proteins without iron-sulfur clusters. Additional studies show that among the housekeeping iron-sulfur cluster assembly proteins encoded by gene cluster *iscSUA-hscBA-fdx-iscX* in *E. coli*, IscU, IscA, and ferredoxin have strong zinc binding activity in *E. coli* cells, and the conserved cysteine residues in the proteins are essential for their zinc binding activity. The deletion of IscU, IscA, and ferredoxin in *E. coli* cells appears to emulate the zinc overload-mediated inhibition of iron-sulfur cluster biogen-

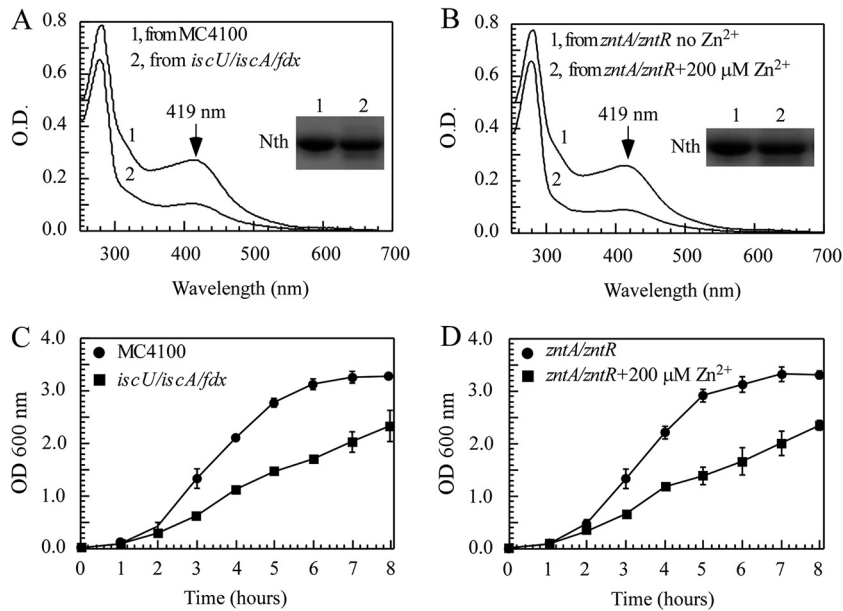


FIG 6 Excess zinc emulates the phenotype of an *E. coli* mutant with deletion of *IscA*, *IscU*, and ferredoxin. (A) UV-visible absorption spectra of recombinant endonuclease III (Nth) purified from *E. coli* MC4100 (spectrum 1) and *iscU iscA fdx* mutant (spectrum 2) in LB medium under aerobic growth conditions. (B) UV-visible absorption spectra of recombinant endonuclease III (Nth) purified from *E. coli zntA zntR* mutant cells (spectrum 1) supplemented with 200 μM ZnSO_4 (spectrum 2) in LB medium under aerobic growth conditions. Insets in panels A and B are photographs of an SDS-PAGE gel of purified proteins. (C) Growth curve of *E. coli iscU iscA fdx* mutant (closed squares) and wild type *E. coli* MC4100 (closed circles) in LB medium under aerobic growth conditions. The results represent the average \pm standard deviation from three independent experiments. (D) Growth curve of *E. coli zntA zntR* mutant supplemented (closed squares) or not (closed circles) with 200 μM ZnSO_4 in LB medium under aerobic growth conditions. The results represent the average \pm standard deviation from three independent experiments.

esis and the slow-growth phenotype of the *E. coli zntA zntR* mutant cells. The results suggest that zinc overload inhibits iron-sulfur cluster biogenesis by specifically targeting *IscU*, *IscA*, and ferredoxin in cells.

Iron-sulfur clusters in proteins are generally vulnerable to reactive oxygen species (51) and nitric oxide (53). Recently, it has also been shown that iron-sulfur clusters in dehydratases are sensitive to copper (54), zinc, and silver (22). Here, we find that iron-sulfur proteins, including fumarases A and B, endonuclease III, biotin synthase, and endogenous NADH dehydrogenase I, are readily inactivated by zinc overload in *E. coli* cells. On the other hand, the preassembled iron-sulfur clusters in proteins are not disrupted by zinc overload in the cells. Thus, zinc overload appears to target iron-sulfur cluster biogenesis instead of disrupting iron-sulfur clusters in proteins in cells. This notion of zinc toxicity is analogous to that of copper toxicity, which also inhibits iron-sulfur cluster biogenesis without affecting preassembled iron-sulfur clusters in cells (48, 55).

One finding of this study is that zinc can effectively inhibit the enzyme activity of NADH dehydrogenase I in the *E. coli zntA zntR* double-mutant cells. This is partially in agreement with the previous observation that zinc inhibits the respiratory chain by both respiratory oxidases (56, 57) and NADH dehydrogenase (57) in *E. coli*. However, we also find that the activity of preexisted NADH dehydrogenase I is not affected significantly by zinc in *E. coli zntA zntR* double-mutant cells. The apparent contradiction with the previous report that zinc inhibits NADH dehydratase directly *in vitro* (57) is likely due to the different experimental conditions. A possible consideration is that the activity of NADH dehydrogenase is sensitive to zinc by determination *in vitro*. In our experiment, prior to the determination of NADH dehydratase I activity, most of the residual zinc after treatment was removed by washing cells twice with buffer. When we measured the activity of NADH dehydratase I, there was little or no zinc in the reaction solution. The activity of the NADH dehydratase I should be unaffected as long as the complex and the bound iron-sulfur clusters are

completely assembled and not destroyed by zinc treated in living cells. Altogether, zinc may not only inhibit the activity of NADH oxidase and quinol oxidases directly but also decrease NADH dehydratase I activity by blocking the iron-sulfur cluster assembly in the enzyme complex in *E. coli* cells.

The effects of high zinc content on wild-type *E. coli* cells have been extensively investigated by transcriptomics (13), proteomics (58) and metalloproteomics (59) approaches. In response to the elevated intracellular zinc content, the cells will express multiple proteins, including ZraP, a putative zinc storage protein (59), a major zinc efflux system, ZntA, a P-type ATPase transporter, and a transcription factor, ZntR (40), among others. When ZntA and ZntR are deleted, the *E. coli* mutant cells accumulate intracellular zinc content, resulting in zinc overload. Because zinc and the iron-sulfur cluster have similar ligand coordination in proteins, it is conceivable that zinc overloading in cells may compete with iron or iron-sulfur cluster binding in the proteins and inhibit iron-sulfur cluster biogenesis in cells. With the exception of IscS, the major iron-sulfur cluster assembly proteins have either iron or iron-sulfur cluster binding sites. Here, we found that zinc overload in the *E. coli zntA zntR* mutant cells inhibits iron-sulfur cluster biogenesis by specifically binding to IscU, IscA, and ferredoxin. The zinc binding in the iron-sulfur cluster assembly protein IscU has previously been reported (60), which is consistent with our results. It may be envisioned that zinc overload forces IscU to bind zinc, which would prevent IscU from assembling iron-sulfur clusters. Zinc binding in IscA has not been previously reported. In the crystal structure, Cys-99 and Cys-101 of IscA are not visible, likely because of their flexible structure (61, 62). Nevertheless, it has been postulated that IscA may form a cysteine pocket with Cys-99 and Cys-101, which are responsible for binding iron (63) and facilitate the binding of other transition metal ions, such as copper or zinc. Our previous study showed that excess copper in *E. coli* cells does lead to copper binding in IscA under aerobic (48) and anaerobic (55) growth conditions and inhibits iron-sulfur cluster assembly. Here, we found that zinc overload in *E. coli* cells results in zinc binding in IscA and blocks iron-sulfur cluster biogenesis. Similarly, ferredoxin hosts a [2Fe-2S] cluster via four cysteine residues (Cys-42, Cys-48, Cys-51, and Cys-87) (64), and zinc overload in *E. coli* cells leads to zinc binding in ferredoxin. Since mutations of the conserved cysteine residues in IscU, IscA, and ferredoxin almost abolish the zinc binding activity of the proteins, these residues are critical for both iron/iron-sulfur clusters and zinc binding in the proteins. We propose that zinc overload in cells results in zinc binding in IscU, IscA, and ferredoxin and inhibits iron-sulfur cluster biogenesis in *E. coli* cells.

Since iron-sulfur proteins are involved in diverse physiological processes ranging from energy metabolism to DNA repair and replication (65), the inhibition of iron-sulfur cluster biogenesis by zinc will have a broad impact on diverse cellular functions. It should be pointed out that iron-sulfur proteins are also the targets of cobalt (66) and copper (48, 54, 55, 67, 68) toxicity. Thus, iron-sulfur cluster biogenesis could be the primary target of heavy-metal toxicity in cells.

MATERIALS AND METHODS

Gene knockout in *E. coli* cells. ZntA and ZntR, two major proteins regulating intracellular zinc homeostasis, were deleted from wild-type *E. coli* (MC4100) following procedures described previously (69). The constructed *E. coli zntA zntR* mutant cells grow normally in LB medium but become hypersensitive to zinc in the medium as reported by Binet and Poole (41). Genes encoding IscU, IscA, and ferredoxin were also deleted from wild-type *E. coli* cells (MC4100). The gene deletion was confirmed by PCR. All primers for the gene deletion and confirmation were synthesized by TaKaRa Co. (Dalian, China).

Protein expression and purification. Genes encoding fumarases A, B, and C from *E. coli* were amplified using PCR and cloned to an expression plasmid, pBAD, as described previously (55). The plasmids expressing *E. coli* IscS, IscU, IscA, HscB, HscA, ferredoxin, IscX, dihydroxy-acid dehydratase (IlvD), endonuclease III (Nth), and biotin synthetase (BioB) were previously prepared. Each plasmid was introduced into the *E. coli zntA zntR* mutant cells. Cells containing the expression plasmid were grown to an optical density at 600 nm (OD_{600}) of 0.6. $ZnSO_4$ was then added to Luria-Bertani (LB) medium 10 min before recombinant protein was induced with 0.02% arabinose at 37°C for 4 h with aeration. Cells were harvested and washed twice with protein purification buffer (NaCl [500 mM], Tris [20 mM, pH 8.0]). Proteins were purified as described previously (55). The purity of purified protein was judged from

TABLE 2 PCR primers used in this work

Primer	Sequence ^a
IscU-C37S-1	ATGGTGGGGGACCGGCTCTGGCGACGTGATG
IscU-C37S-2	GAGGCCGGTGCCCCACCATGCCGCTG
IscU-C63S-1	CGTTTTAAAACTTACGGCTCTGGTCCGCTAT
IscU-C63S-2	GAGCCGTAAGTTTTAAAACGCGCGTC
IscU-C106S-1	CCGCCGGTAAAATCACTCTTCTATTCTGG
IscU-C106S-2	GAGTGAATTTTCACCGCGGCAGTT
Fdx-C42S-1	TGAACACGCCCTCTGAAAAATCCTG
Fdx-C42S-2	GAGCGGTGTTCAATCTCGATACCG
Fdx-C48,51S-1	GCTTCTACCACCTCTACTGCATCGTTCGT
Fdx-C48,51S-2	AGAGGTGGTAGAAGCACAGGATTTTTC
Fdx-C87S-1	AGCCGTTAAGCTCTCAGGCGCGGTTAC
Fdx-C87S-2	AGAGCTTAAACGGCTTCCGGCTCCAG

^aThe underlined bases indicate mutation sites.

SDS-PAGE, followed by the Coomassie blue staining. The concentration of purified protein was determined from the absorption peak at 280 nm using the published extinction coefficients.

Site-directed mutagenesis. The plasmid pBAD-IscA-3M was previously constructed. The IscU-3M (C37/63/106S) and ferredoxin-4M (C42/48/51/87S) mutants were constructed by the site-directed mutagenesis. Each of the conserved cysteine residues in the proteins was replaced with serine. PCR primers used in this work are shown in Table 2, and specific mutations were confirmed by direct sequencing.

Enzyme activity assays for fumarases, dihydroxy-acid dehydratase, NADH dehydrogenase I, and cysteine desulfurase. The activities of purified fumarases A, B, and C were measured by monitoring the reaction product (fumaric acid) in a reaction mixture containing 50 mM sodium phosphate (pH 7.4) and 50 mM substrate (malate) at 250 nm using an extinction coefficient of $1.48 \text{ cm}^{-1} \text{ mM}^{-1}$ (55). For dihydroxy-acid dehydratase, activity was measured using DL-2, 3-dihydroxy-isovalerate as the substrate. In the assay, 10 μl purified IlvD was added to 390 μl preincubated solution containing 50 mM Tris (pH 8.0) and 10 mM substrate. The reaction product (keto acids) was monitored at 240 nm using an extinction coefficient of $0.19 \text{ cm}^{-1} \text{ mM}^{-1}$. NADH dehydrogenase I activity of *E. coli* cells was measured following procedures described previously, with some modifications (48). Briefly, the inverted membrane vesicles of *E. coli* cells were prepared by passing the cells through low-temperature ultrahigh-pressure continuous flow cell disrupter (JN-3000 Plus) once. Inverted membrane vesicles were added to the reaction solution containing 20 mM Tris (pH 8.0), NaCl (200 mM), deamino-NADH (100 μM), sodium azide (400 mM), and plumbagin (400 μM). The NADH dehydrogenase I activity was determined by measuring the oxidation of deamino-NADH at 340 nm ($\epsilon = 6.22 \text{ mM}^{-1} \text{ cm}^{-1}$) at room temperature. In this situation, deamino-NADH as a specific substrate for NADH dehydrogenase I provides electrons (47), sodium azide inhibits the terminal cytochrome oxidases (52), and plumbagin abstracts the electrons directly from the NADH dehydrogenase I (59). The cysteine desulfurase activity of *E. coli* IscS was measured by incubating IscS with dithiothreitol (2 mM) and L-cysteine (0.1 mM) at 37°C. The amount of sulfide produced by IscS in the solution was measured according to Siegel's method (70).

Metal content analyses. Total zinc content in protein samples was determined using the zinc indicator PAR [4-(2-pyridylazo)-resorcinol]. The iron content of protein samples was measured according to Fischer's method (71). Zinc and iron contents in protein samples were also analyzed by the inductively coupled plasma-emission spectrometry (ICP-MS). The results from the two methods were very similar to each other.

For total zinc content of *E. coli*, cells was also determined by ICP-MS. Particularly, the *E. coli* *zntA zntR* mutant and its parental wild-type strain MC4100 cells were grown in LB medium supplemented or not with 200 μM ZnSO_4 at 37°C under aerobic conditions. Cells were harvested from 50 ml LB medium by centrifugation when the OD at 600 nm of the cells reached 0.6. The cell pellet was washed twice with 50 ml of 170 mM NaCl, 20 mM Tris-HCl (pH 8.0), and 2 mM EDTA, resuspended in 5 ml of 170 mM NaCl, and transferred to a microwave digestion vessel with 4 ml nitric acid (35% [vol/vol], Shanghai Yiqian Technology Co. Ltd.) added. The vessel was sealed and placed in the microwave chamber. The following steps were run: the temperature was ramped to 120°C, held for 1 min, ramped to 160°C, held for 6 min, ramped to 180°C, held for 20 min, and reduced to room temperature over 30 min. Once digestion was complete, the samples were diluted using deionized water. The zinc content of above-mentioned samples was determined by ICP-MS.

SUPPLEMENTAL MATERIAL

Supplemental material for this article may be found at <https://doi.org/10.1128/AEM.01967-18>.

SUPPLEMENTAL FILE 1, PDF file, 0.2 MB.

ACKNOWLEDGMENTS

This work was supported by the National Natural Science Foundation of China (grants 81671124, 31629003, 31870775, and 81500440), Key Discipline of Zhejiang Province in

Medical Technology (first class, category A), and College Students in Zhejiang Province Science and Technology Innovation Activity Plan (grant 2018R413187).

REFERENCES

- Roohani N, Hurrell R, Kelishadi R, Schulin R. 2013. Zinc and its importance for human health: an integrative review. *J Res Med Sci* 18:144–157.
- Fukada T, Yamasaki S, Nishida K, Murakami M, Hirano T. 2011. Zinc homeostasis and signaling in health and diseases: zinc signaling. *J Biol Inorg Chem* 16:1123–1134. <https://doi.org/10.1007/s00775-011-0797-4>.
- Prasad AS. 2013. Discovery of human zinc deficiency: its impact on human health and disease. *Adv Nutr* 4:176–190. <https://doi.org/10.3945/an.112.003210>.
- Lemire J, Mailloux R, Appanna VD. 2008. Zinc toxicity alters mitochondrial metabolism and leads to decreased ATP production in hepatocytes. *J Appl Toxicol* 28:175–182. <https://doi.org/10.1002/jat.1263>.
- Sheline CT, Behrens MM, Choi DW. 2000. Zinc-induced cortical neuronal death: contribution of energy failure attributable to loss of NAD(+) and inhibition of glycolysis. *J Neurosci* 20:3139–3146. <https://doi.org/10.1523/JNEUROSCI.20-09-03139.2000>.
- Sharpley MS, Hirst J. 2006. The inhibition of mitochondrial complex I (NADH:ubiquinone oxidoreductase) by Zn²⁺. *J Biol Chem* 281:34803–34809. <https://doi.org/10.1074/jbc.M607389200>.
- Duce JA, Tsatsanis A, Cater MA, James SA, Robb E, Wikke K, Leong SL, Perez K, Johanssen T, Greenough MA, Cho HH, Galatis D, Moir RD, Masters CL, McLean C, Tanzi RE, Cappai R, Barnham KJ, Ciccotosto GD, Rogers JT, Bush AI. 2010. Iron-export ferroxidase activity of beta-amyloid precursor protein is inhibited by zinc in Alzheimer's disease. *Cell* 142:857–867. <https://doi.org/10.1016/j.cell.2010.08.014>.
- Tsunemi T, Krainc D. 2014. Zn²⁺ dyshomeostasis caused by loss of ATP13A2/PARK9 leads to lysosomal dysfunction and alpha-synuclein accumulation. *Hum Mol Genet* 23:2791–2801. <https://doi.org/10.1093/hmg/ddt572>.
- Oутten CE, O'Halloran TV. 2001. Femtomolar sensitivity of metalloregulatory proteins controlling zinc homeostasis. *Science* 292:2488–2492. <https://doi.org/10.1126/science.1060331>.
- Katayama A, Tsujii A, Wada A, Nishino T, Ishihama A. 2002. Systematic search for zinc-binding proteins in *Escherichia coli*. *Eur J Biochem* 269:2403–2413. <https://doi.org/10.1046/j.1432-1033.2002.02900.x>.
- Andreini C, Banci L, Bertini I, Rosato A. 2006. Zinc through the three domains of life. *J Proteome Res* 5:3173–3178. <https://doi.org/10.1021/pr0603699>.
- Brocklehurst KR, Morby AP. 2000. Metal-ion tolerance in *Escherichia coli*: analysis of transcriptional profiles by gene-array technology. *Microbiology* 146:2277–2282. <https://doi.org/10.1099/00221287-146-9-2277>.
- Lee LJ, Barrett JA, Poole RK. 2005. Genome-wide transcriptional response of chemostat-cultured *Escherichia coli* to zinc. *J Bacteriol* 187:1124–1134. <https://doi.org/10.1128/JB.187.3.1124-1134.2005>.
- Ong CL, Gillen CM, Barnett TC, Walker MJ, McEwan AG. 2014. An antimicrobial role for zinc in innate immune defense against group A streptococcus. *J Infect Dis* 209:1500–1508. <https://doi.org/10.1093/infdis/jiu053>.
- Kapetanovic R, Bokil NJ, Achard ME, Ong CL, Peters KM, Stocks CJ, Phan MD, Monteleone M, Schroder K, Irvine KM, Saunders BM, Walker MJ, Stacey KJ, McEwan AG, Schembri MA, Sweet MJ. 2016. Salmonella employs multiple mechanisms to subvert the TLR-inducible zinc-mediated antimicrobial response of human macrophages. *FASEB J* 30:1901–1912. <https://doi.org/10.1096/fj.201500061>.
- Abrantes MC, Kok J, Silva Lopes MDF. 2014. Enterococcus faecalis zinc-responsive proteins mediate bacterial defence against zinc overload, lysozyme and oxidative stress. *Microbiology* 160:2755–2762. <https://doi.org/10.1099/mic.0.080341-0>.
- Lu J, Wang W, Tan G, Landry AP, Yi P, Si F, Ren Y, Ding H. 2011. *Escherichia coli* topoisomerase I is an iron and zinc binding protein. *Biometals* 24:729–736. <https://doi.org/10.1007/s10534-011-9425-6>.
- Wang W, Su X, Wang X, Yang J, Zhang T, Wang M, Wan R, Tan G, Lu J. 2014. Iron inhibits *Escherichia coli* topoisomerase I activity by targeting the first two zinc-binding sites in the C-terminal domain. *Protein Sci* 23:1619–1628. <https://doi.org/10.1002/pro.2542>.
- Cheng Z, Tan G, Wang W, Su X, Landry AP, Lu J, Ding H. 2014. Iron and zinc binding activity of *Escherichia coli* topoisomerase I homolog YrdD. *Biometals* 27:229–236. <https://doi.org/10.1007/s10534-013-9698-z>.
- Wiley SE, Paddock ML, Abresch EC, Gross L, van der Geer P, Nechushtai R, Murphy AN, Jennings PA, Dixon JE. 2007. The outer mitochondrial membrane protein mitoNEET contains a novel redox-active 2Fe-2S cluster. *J Biol Chem* 282:23745–23749. <https://doi.org/10.1074/jbc.C700107200>.
- Shimberg GD, Michalek JL, Oluyadi AA, Rodrigues AV, Zucconi BE, Neu HM, Ghosh S, Sureschandra K, Wilson GM, Stemmler TL, Michel SL. 2016. Cleavage and polyadenylation specificity factor 30: An RNA-binding zinc-finger protein with an unexpected 2Fe-2S cluster. *Proc Natl Acad Sci U S A* 113:4700–4705. <https://doi.org/10.1073/pnas.1517620113>.
- Xu FF, Imlay JA. 2012. Silver(I), mercury(II), cadmium(II), and zinc(II) target exposed enzymic iron-sulfur clusters when they toxify *Escherichia coli*. *Appl Environ Microbiol* 78:3614–3621. <https://doi.org/10.1128/AEM.07368-11>.
- Tan G, Landry AP, Dai R, Wang L, Lu J, Ding H. 2012. Competition of zinc ion for the [2Fe-2S] cluster binding site in the diabetes drug target protein mitoNEET. *Biometals* 25:1177–1184. <https://doi.org/10.1007/s10534-012-9580-4>.
- Iannuzzi C, Adrover M, Puglisi R, Yan R, Temussi PA, Pastore A. 2014. The role of zinc in the stability of the marginally stable IscU scaffold protein. *Protein Sci* 23:1208–1219. <https://doi.org/10.1002/pro.2501>.
- Wachnowsky C, Fidai I, Cowan JA. 2018. Iron-sulfur cluster biosynthesis and trafficking—impact on human disease conditions. *Metallomics* 10:9–29. <https://doi.org/10.1039/c7mt00180k>.
- Zheng L, Cash VL, Flint DH, Dean DR. 1998. Assembly of iron-sulfur clusters. Identification of an iscSUA-hscBA-fox gene cluster from *Azotobacter vinelandii*. *J Biol Chem* 273:13264–13272. <https://doi.org/10.1074/jbc.273.21.13264>.
- Cupp-Vickery JR, Urbina H, Vickery LE. 2003. Crystal structure of IscS, a cysteine desulfurase from *Escherichia coli*. *J Mol Biol* 330:1049–1059. [https://doi.org/10.1016/S0022-2836\(03\)00690-9](https://doi.org/10.1016/S0022-2836(03)00690-9).
- Marinoni EN, de Oliveira JS, Nicolet Y, Raulfs EC, Amara P, Dean DR, Fontecilla-Camps JC. 2012. (IscS-IscU)₂ complex structures provide insights into Fe₂S₂ biogenesis and transfer. *Angew Chem Int Ed Engl* 51:5439–5442. <https://doi.org/10.1002/anie.201201708>.
- Yan R, Kelly G, Pastore A. 2014. The scaffold protein IscU retains a structured conformation in the Fe-S cluster assembly complex. *ChemBiochem* 15:1682–1686. <https://doi.org/10.1002/cbic.201402211>.
- Unciuleac MC, Chandramouli K, Naik S, Mayer S, Huynh BH, Johnson MK, Dean DR. 2007. In vitro activation of apo-aconitase using a [4Fe-4S] cluster-loaded form of the IscU [Fe-S] cluster scaffolding protein. *Biochemistry* 46:6812–6821. <https://doi.org/10.1021/bi0626665>.
- Brancaccio D, Gallo A, Mikolajczyk M, Zovo K, Palumaa P, Novellino E, Piccoli M, Ciofi-Baffoni S, Banci L. 2014. Formation of [4Fe-4S] clusters in the mitochondrial iron-sulfur cluster assembly machinery. *J Am Chem Soc* 136:16240–16250. <https://doi.org/10.1021/ja507822j>.
- Mapolelo DT, Zhang B, Naik SG, Huynh BH, Johnson MK. 2012. Spectroscopic and functional characterization of iron-bound forms of *Azotobacter vinelandii* (Nif)IscA. *Biochemistry* 51:8056–8070. <https://doi.org/10.1021/bi300664j>.
- Yang J, Bitoun JP, Ding H. 2006. Interplay of IscA and IscU in biogenesis of iron-sulfur clusters. *J Biol Chem* 281:27956–27963. <https://doi.org/10.1074/jbc.M601356200>.
- Landry AP, Cheng Z, Ding H. 2013. Iron binding activity is essential for the function of IscA in iron-sulfur cluster biogenesis. *Dalton Trans* 42:3100–3106. <https://doi.org/10.1039/c2dt32000b>.
- Kim JH, Tonelli M, Frederick RO, Chow DC, Markley JL. 2012. Specialized Hsp70 chaperone (HscA) binds preferentially to the disordered form, whereas J-protein (HscB) binds preferentially to the structured form of the iron-sulfur cluster scaffold protein (IscU). *J Biol Chem* 287:31406–31413. <https://doi.org/10.1074/jbc.M112.352617>.
- Kim JH, Frederick RO, Reinen NM, Troupis AT, Markley JL. 2013. [2Fe-2S]Ferrodoxin binds directly to cysteine desulfurase and supplies an electron for iron-sulfur cluster assembly but is displaced by the scaffold protein or bacterial frataxin. *J Am Chem Soc* 135:8117–8120. <https://doi.org/10.1021/ja401950a>.
- Kim JH, Bothe JR, Frederick RO, Holder JC, Markley JL. 2014. Role of IscX in iron-sulfur cluster biogenesis in *Escherichia coli*. *J Am Chem Soc* 136:7933–7942. <https://doi.org/10.1021/ja501260h>.

38. Adinolfi S, Puglisi R, Crack JC, Iannuzzi C, Dal Piaz F, Konarev PV, Svergun DI, Martin S, Le Brun NE, Pastore A. 2017. The molecular bases of the dual regulation of bacterial iron sulfur cluster biogenesis by CyaY and IscX. *Front Mol Biosci* 4:97. <https://doi.org/10.3389/fmolb.2017.00097>.
39. Roche B, Huguenot A, Barras F, Py B. 2015. The iron-binding CyaY and IscX proteins assist the ISC-catalyzed Fe-S biogenesis in *Escherichia coli*. *Mol Microbiol* 95:605–623. <https://doi.org/10.1111/mmi.12888>.
40. Rensing C, Mitra B, Rosen BP. 1997. The zntA gene of *Escherichia coli* encodes a Zn(II)-translocating P-type ATPase. *Proc Natl Acad Sci U S A* 94:14326–14331. <https://doi.org/10.1073/pnas.94.26.14326>.
41. Binet MR, Poole RK. 2000. Cd(II), Pb(II) and Zn(II) ions regulate expression of the metal-transporting P-type ATPase ZntA in *Escherichia coli*. *FEBS Lett* 473:67–70. [https://doi.org/10.1016/S0014-5793\(00\)01509-X](https://doi.org/10.1016/S0014-5793(00)01509-X).
42. van Vugt-Lussenburg BM, van der Weel L, Hagen WR, Hagedoorn PL. 2013. Biochemical similarities and differences between the catalytic [4Fe-4S] cluster containing fumarases FumA and FumB from *Escherichia coli*. *PLoS One* 8:e55549. <https://doi.org/10.1371/journal.pone.0055549>.
43. Weaver T. 2005. Structure of free fumarase C from *Escherichia coli*. *Acta Crystallogr D Biol Crystallogr* 61:1395–1401. <https://doi.org/10.1107/S0907444905024194>.
44. Lotierzo M, Bui BT, Leech HK, Warren MJ, Marquet A, Rigby SE. 2009. Iron-sulfur cluster dynamics in biotin synthase: a new [2Fe-2S]¹⁺ cluster. *Biochem Biophys Res Commun* 381:487–490. <https://doi.org/10.1016/j.bbrc.2009.02.089>.
45. Fugate CJ, Jarrett JT. 2012. Biotin synthase: insights into radical-mediated carbon-sulfur bond formation. *Biochim Biophys Acta* 1824:1213–1222. <https://doi.org/10.1016/j.bbapap.2012.01.010>.
46. Berrisford JM, Baradaran R, Sazanov LA. 2016. Structure of bacterial respiratory complex I. *Biochim Biophys Acta* 1857:892–901. <https://doi.org/10.1016/j.bbabbio.2016.01.012>.
47. Matsushita K, Ohnishi T, Kaback HR. 1987. NADH-ubiquinone oxidoreductases of the *Escherichia coli* aerobic respiratory chain. *Biochemistry* 26:7732–7737. <https://doi.org/10.1021/bi00398a029>.
48. Tan G, Cheng Z, Pang Y, Landry AP, Li J, Lu J, Ding H. 2014. Copper binding in IscA inhibits iron-sulphur cluster assembly in *Escherichia coli*. *Mol Microbiol* 93:629–644. <https://doi.org/10.1111/mmi.12676>.
49. Flint DH, Emptage MH, Finnegan MG, Fu W, Johnson MK. 1993. The role and properties of the iron-sulfur cluster in *Escherichia coli* dihydroxy-acid dehydratase. *J Biol Chem* 268:14732–14742.
50. Boal AK, Yavin E, Lukianova OA, O'Shea VL, David SS, Barton JK. 2005. DNA-bound redox activity of DNA repair glycosylases containing [4Fe-4S] clusters. *Biochemistry* 44:8397–8407. <https://doi.org/10.1021/bi047494n>.
51. Jang S, Imlay JA. 2010. Hydrogen peroxide inactivates the *Escherichia coli* Isc iron-sulphur assembly system, and OxyR induces the Suf system to compensate. *Mol Microbiol* 78:1448–1467. <https://doi.org/10.1111/j.1365-2958.2010.07418.x>.
52. Green GN, Kranz RG, Lorence RM, Gennis RB. 1984. Identification of subunit I as the cytochrome b558 component of the cytochrome d terminal oxidase complex of *Escherichia coli*. *J Biol Chem* 259:7994–7997.
53. Ren B, Zhang N, Yang J, Ding H. 2008. Nitric oxide-induced bacteriostasis and modification of iron-sulphur proteins in *Escherichia coli*. *Mol Microbiol* 70:953–964. <https://doi.org/10.1111/j.1365-2958.2008.06464.x>.
54. Macomber L, Imlay JA. 2009. The iron-sulfur clusters of dehydratases are primary intracellular targets of copper toxicity. *Proc Natl Acad Sci U S A* 106:8344–8349. <https://doi.org/10.1073/pnas.0812808106>.
55. Tan GQ, Yang J, Li T, Zhao J, Sun SJ, Li XK, Lin CX, Li JH, Zhou HB, Lyu JX, Dinga HG. 2017. Anaerobic copper toxicity and iron-sulfur cluster biogenesis in *Escherichia coli*. *Appl Environ Microbiol* 83:e00867-17. <https://doi.org/10.1128/AEM.00867-17>.
56. Poole RK, Williams HD, Downie JA, Gibson F. 1989. Mutations affecting the cytochrome d-containing oxidase complex of *Escherichia coli* K12: identification and mapping of a fourth locus, cydD. *J Gen Microbiol* 135:1865–1874. <https://doi.org/10.1099/00221287-135-7-1865>.
57. Beard SJ, Hughes MN, Poole RK. 1995. Inhibition of the cytochrome bd-terminated NADH oxidase system in *Escherichia coli* K-12 by divalent metal cations. *FEMS Microbiol Lett* 131:205–210. <https://doi.org/10.1111/j.1574-6968.1995.tb07778.x>.
58. Easton JA, Thompson P, Crowder MW. 2006. Time-dependent translational response of *E. coli* to excess Zn(II). *J Biomol Tech* 17:303–307.
59. Korshunov S, Imlay KR, Imlay JA. 2016. The cytochrome bd oxidase of *Escherichia coli* prevents respiratory inhibition by endogenous and exogenous hydrogen sulfide. *Mol Microbiol* 101:62–77. <https://doi.org/10.1111/mmi.13372>.
60. Ramelot TA, Cort JR, Goldsmith-Fischman S, Kornhaber GJ, Xiao R, Shastry R, Acton TB, Honig B, Montelione GT, Kennedy MA. 2004. Solution NMR structure of the iron-sulfur cluster assembly protein U (IscU) with zinc bound at the active site. *J Mol Biol* 344:567–583. <https://doi.org/10.1016/j.jmb.2004.08.038>.
61. Bilder PW, Ding H, Newcomer ME. 2004. Crystal structure of the ancient, Fe-S scaffold IscA reveals a novel protein fold. *Biochemistry* 43:133–139. <https://doi.org/10.1021/bi035440s>.
62. Cupp-Vickery JR, Silberg JJ, Ta DT, Vickery LE. 2004. Crystal structure of IscA, an iron-sulfur cluster assembly protein from *Escherichia coli*. *J Mol Biol* 338:127–137. <https://doi.org/10.1016/j.jmb.2004.02.027>.
63. Ding H, Clark RJ. 2004. Characterization of iron binding in IscA, an ancient iron-sulphur cluster assembly protein. *Biochem J* 379:433–440. <https://doi.org/10.1042/BJ20031702>.
64. Kakuta Y, Horio T, Takahashi Y, Fukuyama K. 2001. Crystal structure of *Escherichia coli* Fdx, an adrenodoxin-type ferredoxin involved in the assembly of iron-sulfur clusters. *Biochemistry* 40:11007–11012. <https://doi.org/10.1021/bi010544t>.
65. Lill R. 2009. Function and biogenesis of iron-sulphur proteins. *Nature* 460:831–838. <https://doi.org/10.1038/nature08301>.
66. Ranquet C, Ollagnier-de-Choudens S, Loiseau L, Barras F, Fontecave M. 2007. Cobalt stress in *Escherichia coli*. The effect on the iron-sulfur proteins. *J Biol Chem* 282:30442–30451. <https://doi.org/10.1074/jbc.M702519200>.
67. Chillappagari S, Seubert A, Trip H, Kuipers OP, Marahiel MA, Miethke M. 2010. Copper stress affects iron homeostasis by destabilizing iron-sulfur cluster formation in *Bacillus subtilis*. *J Bacteriol* 192:2512–2524. <https://doi.org/10.1128/JB.00058-10>.
68. Vallières C, Holland SL, Avery SV. 2017. Mitochondrial ferredoxin determines vulnerability of cells to copper excess. *Cell Chem Biol* 24:1228–1237.e1223. doi: <https://doi.org/10.1016/j.chembiol.2017.08.005>.
69. Lu J, Yang J, Tan G, Ding H. 2008. Complementary roles of SufA and IscA in the biogenesis of iron-sulfur clusters in *Escherichia coli*. *Biochem J* 409:535–543. <https://doi.org/10.1042/BJ20071166>.
70. Siegel LM. 1965. A direct microdetermination for sulfide. *Anal Biochem* 11:126–132. [https://doi.org/10.1016/0003-2697\(65\)90051-5](https://doi.org/10.1016/0003-2697(65)90051-5).
71. Fischer DS. 1967. A method for the rapid detection of acute iron toxicity. *Clin Chem* 13:6–11.